

# Mechanistic Investigations on E–N Bond-Breaking and Ring Expansion for *N*-Heterocyclic Carbene Analogues Containing the Group 14 Elements (E)

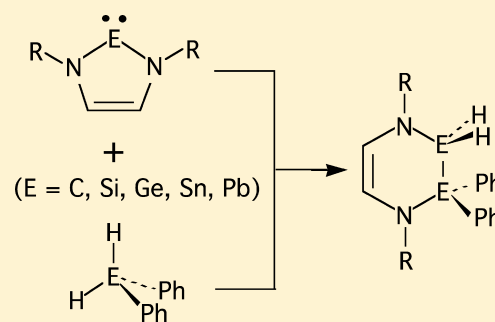
Ming-Der Su\*

Department of Applied Chemistry, National Chiayi University, Chiayi 60004, Taiwan

Department of Medicinal and Applied Chemistry, Kaohsiung Medical University, Kaohsiung 80708, Taiwan

## Supporting Information

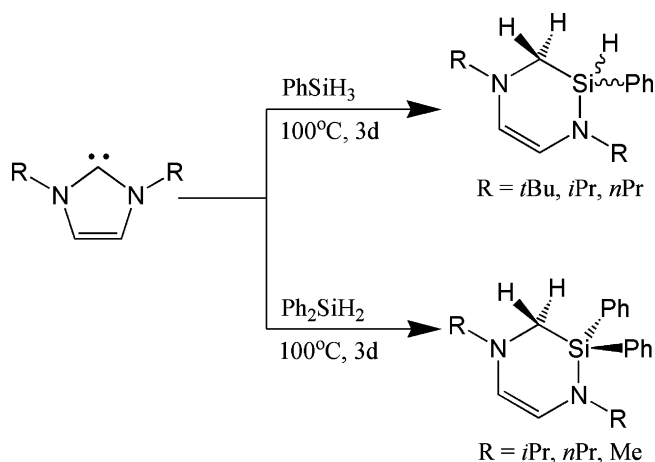
**ABSTRACT:** The potential-energy surfaces for the ring-expansion reactions  ${}^i\text{PrN}(\text{CH})_2\text{N}({}^i\text{Pr})\text{E}:(\text{Rea}-\text{E}) + \text{SiH}_2\text{Ph}_2 \rightarrow$  six-membered ring heterocyclic product ( $\text{E} = \text{C}, \text{Si}, \text{Ge}, \text{Sn}, \text{and Pb}$ ) and  ${}^i\text{PrN}(\text{CH})_2\text{N}({}^i\text{Pr})\text{C}:(\text{Rea}-\text{C}) + \text{EH}_2\text{Ph}_2 \rightarrow$  six-membered ring heterocyclic product are studied at the M06-2X/Def2-TZVP level of theory. These theoretical investigations suggest that for a given  $\text{SiH}_2\text{Ph}_2$ , the relative reactivity of  $\text{Rea}-\text{E}$  toward the ring-expansion reaction decreases as the atomic weight of the central atom E increases, that is, in the order  $\text{Rea}-\text{C} \gg \text{Rea}-\text{Si} > \text{Rea}-\text{Ge} > \text{Rea}-\text{Sn} > \text{Rea}-\text{Pb}$ . However, for a given  $\text{Rea}-\text{C}$ , these theoretical observations demonstrate that the reactivity of the  $\text{EH}_2\text{Ph}_2$  molecule that undergoes the ring-expansion reaction decreases in the order  $\text{SiH}_2\text{Ph}_2 \approx \text{GeH}_2\text{Ph}_2 \approx \text{SnH}_2\text{Ph}_2 > \text{PbH}_2\text{Ph}_2 \gg \text{CH}_2\text{Ph}_2$ . This theoretical study indicates that both the electronic structure and steric effects play a crucial role in determining their reactivities. The model conclusions are consistent with available experimental findings. Furthermore, a valence bond state correlation diagram model can be used to rationalize the computational results. These results allow a number of predictions to be made.



## I. INTRODUCTION

Recently, Radius<sup>1</sup> and co-workers reported some surprising reactions for the stable 1,3-dialkylimidazolin-2-ylidenes (NHCs) with hydrosilanes, which lead to six-membered heterocycles (see Scheme 1). In these reactions, different NHCs ( $\text{RN}(\text{CH})_2\text{N}(\text{R})\text{C}:$ ;  $\text{Rea}-\text{E}$ ,  $\text{E} = \text{C}, \text{Si}, \text{Ge}, \text{Sn}, \text{and Pb}$ ) have been found to react with  $\text{PhSiH}_3$  and  $\text{Ph}_2\text{SiH}_2$  to yield 3,4-dehydro-2,5-diazasilanes. It was structurally confirmed that two hydrogen atoms transfer from

Scheme 1



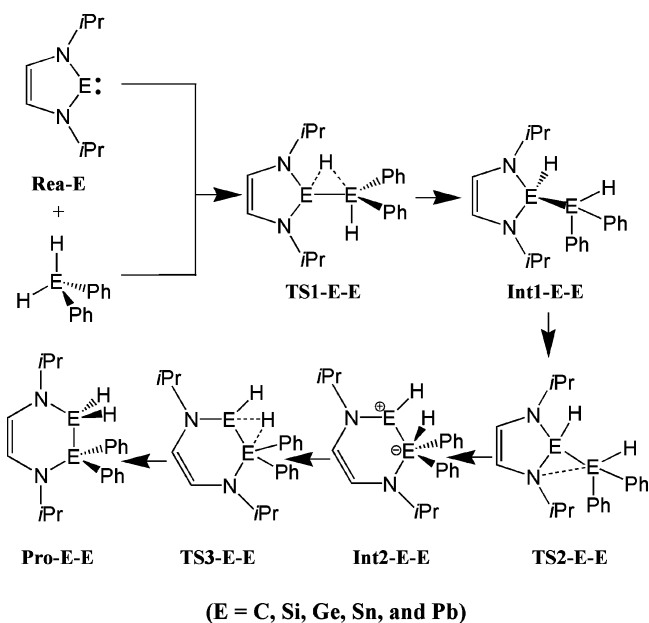
phenylsilane (or diphenylsilane) to the NHC carbon atom, with the insertion of the remaining silylene moiety into one of the C–N bonds of NHC, to produce a six-membered heterocyclic product.<sup>4</sup> On the basis of these experimental findings, Radius and co-workers proposed one possible mechanism for the process of ring expansion for an NHC (Scheme 2).<sup>1</sup> In the first step of the reaction, the stable NHC ( $\text{Rea}-\text{C}$ ) carbon atom inserts into the H–Si bond of the silane to give an intermediate ( $\text{Int1}-\text{C}-\text{Si}$ ), followed by amide transfer to the silicon element to produce the second intermediate ( $\text{Int2}-\text{C}-\text{Si}$ ). The final step of the reaction involves the transfer of one hydrogen atom from the silicon atom to the carbon atom to yield the six-membered heterocycle ( $\text{Pro}-\text{C}-\text{Si}$ ).

These intriguing and important results arouse the author's interest. If the NHC can be used to react with hydrosilanes to obtain the ring-expansion products, it may be possible to extend this to other *N*-heterocyclic carbene analogues that feature the group 14 elements E, as well as to the hydrocarbons that possess the E atoms. Four theoretical papers have, to the author's knowledge, been published concerning such ring-expansion reactions for NHC systems.<sup>2</sup> We thus believe that a somewhat different approach and emphasis on other aspects of the reaction analyzed here may supplement the general belief.<sup>3</sup>

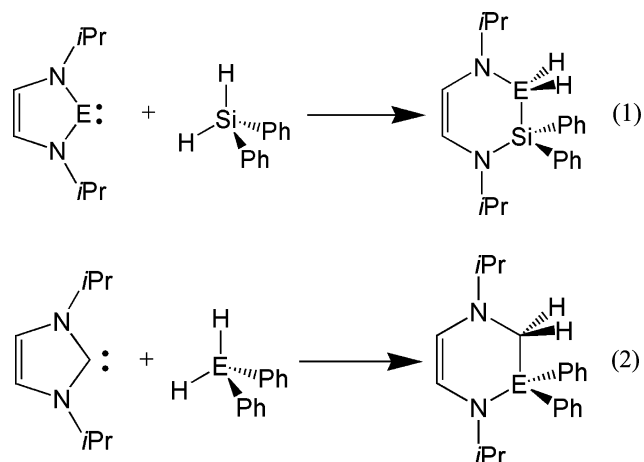
Received: January 23, 2014

Published: May 1, 2014

Scheme 2



The aim in this work is to obtain detailed mechanistic knowledge, to exercise greater control over these reactions. In this Paper, the  $\text{PrN}(\text{CH})_2\text{N}(\text{Pr})\text{E}$ : and  $\text{EH}_2\text{Ph}_2$  systems are chosen as model reactants, to investigate their potential-energy surfaces and the mechanisms of the reactions (see eqs 1 and 2).



It is hoped that these theoretical investigations will provide a better understanding of the thermodynamic and kinetic aspects of such ring-expansion reactions (Scheme 2) and that they will provide an optimal design for further related synthesis and catalytic processes.

## II. THEORETICAL METHODS

Geometries are fully optimized with hybrid density functional theory (DFT) at the M06-2X level of theory, using the Gaussian 09 program package.<sup>6</sup> It was recently reported that M06, a hybrid meta functional, is a functional with good accuracy for most, if not all, transition metals, main-group thermochemistry, medium-range correlation energy, and barrier heights.<sup>7</sup> In particular, M06-2X has been proved to have excellent performance for main-group chemistry.<sup>7</sup> Thus, the geometries of all the stationary points were fully optimized at the M06-2X level of theory.

These M06-2X calculations were carried out with pseudorelativistic effective core potentials on group 14 elements, using the Def2-TZVP basis sets.<sup>8</sup> Accordingly, these M06-2X calculations are denoted as M06-2X/Def2-TZVP. Therefore, the model molecules computed in this work have 924 (190 electrons) basis functions.

Frequency calculations were performed on all of the structures to confirm that the reactants and products have no imaginary frequencies and that the transition states (TSs) possess only one imaginary frequency. The relative energies at 0 K are thus corrected for vibrational zero-point energies (ZPE, not scaled). Thermodynamic corrections to 298 K, ZPE corrections, heat capacity corrections, and entropy corrections ( $\Delta S$ ) obtained are applied at the M06-2X/Def2-TZVP level. Therefore, the relative free energy ( $\Delta G$ ) at 298 K is also calculated at the same level of theory. The Cartesian coordinates calculated for the stationary points at the M06-2X/Def2-TZVP level are available as Supporting Information.

## III. RESULTS AND DISCUSSION

### (1). Geometries and Electronic Structures of Rea-E. In

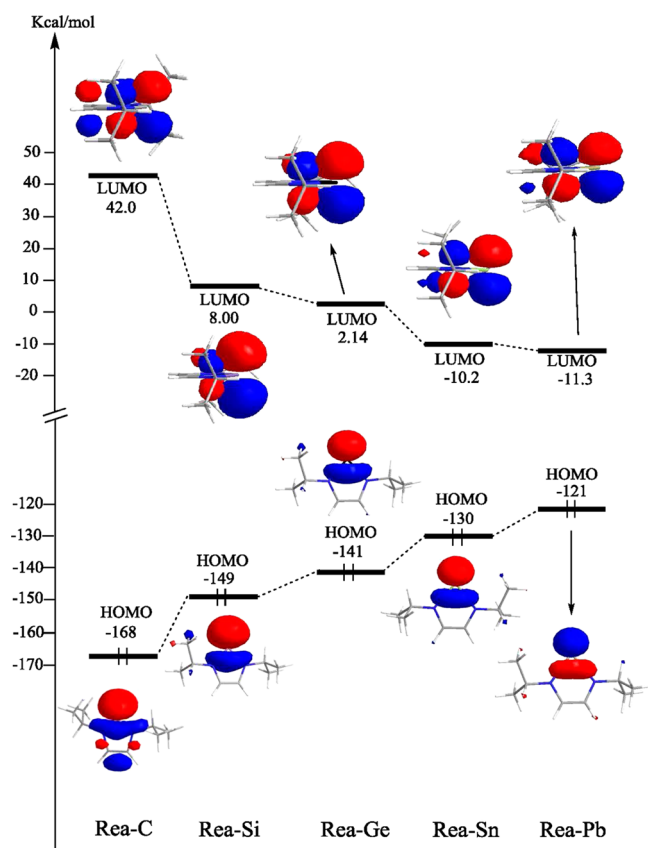
this work, the reactants Rea-E ( $\text{PrN}(\text{CH})_2\text{N}(\text{Pr})\text{E}$ :; E = C, Si, Ge, Sn, and Pb) are calculated both as singlet and as triplet species, whose geometric parameters are shown in Table 1.

Table 1. Selected Geometric Values and Relative Energies for Singlet and Triplet Group 14 Carbenic Analogues<sup>a</sup>

system	E = C	E = Si	E = Ge	E = Sn	E = Pb
(singlet)					
E–N (Å)	1.357	1.757	1.873	2.073	2.179
N–C (Å)	1.382	1.382	1.375	1.374	1.366
C–C (Å)	1.350	1.348	1.353	1.356	1.361
$\angle\text{NEN}$ (deg)	109.8	87.22	83.86	78.68	75.80
(triplet)					
E–N (Å)	1.399	1.921	2.055	2.258	2.374
N–C (Å)	1.404	1.325	1.322	1.323	1.323
C–C (Å)	1.338	1.400	1.402	1.404	1.404
$\angle\text{NEN}$ (deg)	102.2	82.24	79.12	75.28	71.74

<sup>a</sup>That is, Rea-E ( $\text{PrN}(\text{CH})_2\text{N}(\text{Pr})\text{E}$ :), where E = C, Si, Ge, Sn, and Pb. All were calculated at the M06-2X/Def2-TZVP (singlet) and UM06-2X/Def2-TZVP (triplet) levels of theory.

Figure 1 is a molecular orbital correlation diagram (in which LUMO = lowest unoccupied molecular orbital and HOMO = highest occupied molecular orbital) of the valence orbitals for Rea-E. It is well-known that traditional carbene species have two key orbitals, namely, the occupied  $\sigma$ -symmetry and the unoccupied  $p-\pi$  orbital.<sup>9</sup> An interesting feature is the singlet–triplet splitting  $\Delta E'_{st}$ . Traditionally,  $\Delta E'_{st}$  is the energy difference between the optimized structures of the singlet and the triplet states ( $= E_{\text{triplet}} - E_{\text{singlet}}$ ). Nevertheless, if we only consider the two key orbitals in the present work, then our M06-2X calculations demonstrate that the new  $\Delta E_{st}$  value (kcal/mol)



**Figure 1.** Calculated frontier MOs for the singlet  $\text{Rea-E}$  ( $(\text{PrN}(\text{CH}_2)_2\text{N}(\text{Pr})\text{E})_2$ ;  $\text{E} = \text{C}, \text{Si}, \text{Ge}, \text{Sn}, \text{and Pb}$ ) species.

increases in the order  $\text{Rea-C}$  (210) <  $\text{Rea-Si}$  (218) <  $\text{Rea-Ge}$  (229) <  $\text{Rea-Sn}$  (233) <  $\text{Rea-Pb}$  (236). In other words, the heavier the central group 14 atom  $\text{E}$ , the larger the  $\Delta E_{\text{st}}$  of a  $\text{Rea-E}$  carbene species. Finally, our M06-2X calculations indicate that the  $\text{Rea-E}$  species all possess a singlet ground state. This strongly indicates that both reactions (eqs 1 and 2) proceed on the singlet surface, so the singlet surface is the focus of this study.

**(2). Geometrical and Energetic Results for eq 1.** As stated previously, the reaction from  $\text{Rea-E}$  to  $\text{Pro-E-E}$  can be considered as a ring expansion of the five-membered ring

species<sup>5</sup> to the six-membered heterocycle by the incorporation of one molecule of  $\text{SiH}_2\text{Ph}_2$ . It is predicted that the expansion mechanism is as illustrated in Scheme 2. Namely, the following reaction mechanism is used to explore the  $\text{N-E}$  bond cleavage and ring expansion of NHCs, using  $\text{SiH}_2\text{Ph}_2$  (eq 1):  $\text{Rea-E} + \text{SiH}_2\text{Ph}_2 \rightarrow \text{TS1-E-Si} \rightarrow \text{Int1-E-Si} \rightarrow \text{TS2-E-Si} \rightarrow \text{Int2-E-Si} \rightarrow \text{TS3-E-Si} \rightarrow \text{Pro-E-Si}$  (Scheme 2). For the systems  $\text{TS1-E-Si}$ ,  $\text{Int1-E-Si}$ ,  $\text{TS2-E-Si}$ ,  $\text{Int2-E-Si}$ ,  $\text{TS3-E-Si}$ , and  $\text{Pro-E-Si}$ , the geometries and energetics were calculated using the M06-2X/Def2-TZVP level of theory. The relative Gibbs free energies of the stationary points for this mechanism are shown in Table 2 and Figure 2. Selected geometrical parameters for the structure of stationary points are shown in the Supporting Information (Figures A–F, respectively). The major conclusions to be drawn from this study can be summarized as follows.

(a) From Table 2 and Figure 2, it is apparent that the heavier the atomic number of the group 14  $\text{E}$  atom involved in eq 1, the larger is the activation energy for the ring-expansion process. For instance, since the atomic weight of the group 14  $\text{E}$  atom increases in the order  $\text{C} < \text{Si} < \text{Ge} < \text{Sn} < \text{Pb}$ , the Gibbs free activation energy for the transition from reactants to  $\text{TS1-E-Si}$  increases in the same order. A similar phenomenon is also found for the cases of both  $\text{TS2-E-Si}$  and  $\text{TS3-E-Si}$ . It is also noteworthy that in the same group 14  $\text{E}$  element reaction, the activation barrier for  $\text{TS1-E-Si}$  is fundamentally much larger than that for both  $\text{TS2-E-Si}$  and  $\text{TS3-E-Si}$ , except for the case of the  $\text{Rea-Si}$  species. This strongly indicates that the  $\text{TS1-E-Si}$  is the important rate-determining step for the entire ring-expansion process of eq 1 (vide infra).

(b) As previously mentioned in eq 1, there are two types of intermediates, namely,  $\text{Int1-E-Si}$  and  $\text{Int2-E-Si}$ , whose computed geometrical structures are given in the Supporting Information (Figures B and D, respectively). The calculated vibrational frequencies for these intermediates demonstrate that these structures are true minima on the potential-energy surface of the ring-expansion reaction (eq 1). As expected, these intermediates all display the five-membered ring ( $\text{Int1-E-Si}$ ) and six-membered ring ( $\text{Int2-E-Si}$ ) bonding characteristics. As seen in the Supporting Information (Figure B), the  $\text{E-Si}$  bond length in the  $\text{Int1-E-Si}$  species increases as the atomic weight of the atom  $\text{E}$  increases. The same effect is also seen for

**Table 2.** Relative Energies (kcal/mol) for the Process Illustrated in Scheme 2<sup>a,b</sup>

system	$\text{E} = \text{C}$	$\text{E} = \text{Si}$	$\text{E} = \text{Ge}$	$\text{E} = \text{Sn}$	$\text{E} = \text{Pb}$
$\text{Rea-E} + \text{SiH}_2\text{Ph}_2$	0.0	0.0	0.0	0.0	0.0
$\text{TS1-E-Si}$ ( $\Delta E_{\text{TS1}}$ )	+35.7 (+20.6)	+39.5 (+27.3)	+48.8 (+34.8)	+59.5 (+43.5)	+76.4 (+63.4)
$\text{Int1-E-Si}$ ( $\Delta E_{\text{Int1}}$ )	+4.15 (-9.22)	+4.72 (-10.1)	+17.2 (+4.00)	+31.1 (+17.0)	+56.9 (+42.9)
$\text{TS2-E-Si}$ ( $\Delta E_{\text{TS2}}$ )	+28.6 (+15.1)	+38.0 (+24.1)	+43.0 (+28.8)	+52.6 (+36.5)	+67.7 (+50.2)
$\text{Int2-E-Si}$ ( $\Delta E_{\text{Int2}}$ )	+13.8 (-0.176)	+27.7 (+13.1)	+38.8 (+25.7)	+26.7 (+10.8)	+21.9 (+4.39)
$\text{TS3-E-Si}$ ( $\Delta E_{\text{TS3}}$ )	+21.4 (+7.24)	+45.8 (+31.1)	+48.1 (+33.2)	+53.2 (+36.9)	+59.3 (+43.6)
$\text{Pro-E-Si}$ ( $\Delta E_{\text{Pro1}}$ )	-27.3 (-41.9)	+2.41 (-11.7)	+7.74 (-4.98)	+22.6 (+5.60)	+37.4 (+22.9)

<sup>a</sup>That is,  $\text{Rea-C} + \text{EH}_2\text{Ph}_2 \rightarrow \text{TS1-C-E} \rightarrow \text{Int1-C-E} \rightarrow \text{TS2-C-E} \rightarrow \text{Int2-C-E} \rightarrow \text{TS3-C-E} \rightarrow \text{Pro-C-E}$ , calculated at the M06-2X/Def2-TZVP level of theory. For the M06-2X optimized structures of the stationary points, see the Supporting Information (Figures A–F). <sup>b</sup>Gibbs free energy and zero-point energy (in parentheses).

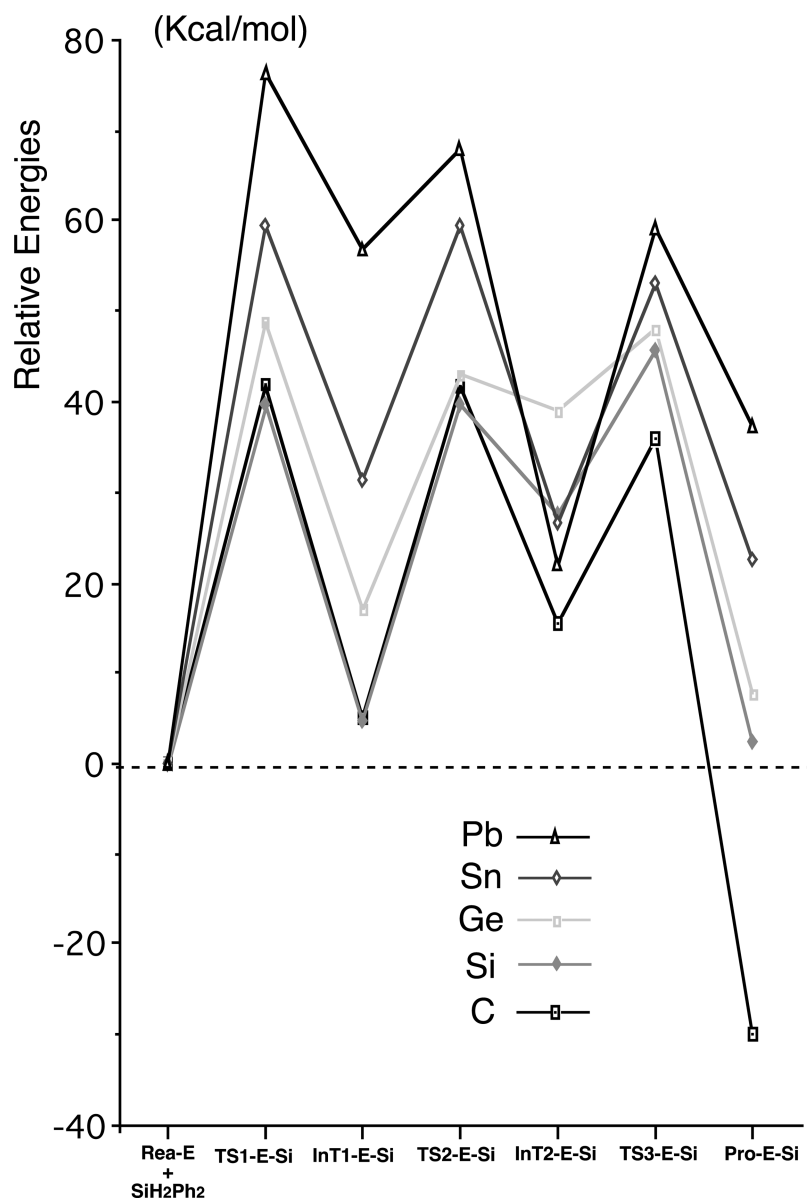


**Figure 2.** The potential-energy surfaces of the reactants **Rea**–**E** +  $\text{SiH}_2\text{Ph}_2$ , transition states, intermediates, and ring-expansion products ( $\text{E} = \text{C}, \text{Si}, \text{Ge}, \text{Sn}, \text{and Pb}$ ), based on the M06-2X/Def2-TZVP calculations. For the relative Gibbs free energies for each species, see Table 2.

the second intermediate, **Int2**–**E**–**Si**, with the six-membered geometry. These findings can be explained in terms of the expected atomic size of the group 14 atom **E**, which increases from **C** to **Pb**.

The most striking results are the geometrical structures of the intermediates **Int2**–**E**–**Si**. As seen in the Supporting Information (Figure D), in all cases the silicon atom is coordinated in a distorted trigonal-bipyramidal geometry<sup>10</sup> that features two carbon atoms from the attached phenyl substituents, one hydrogen atom and, from the supporting NHC group, one **E** atom and one nitrogen atom. The structural index  $\tau$ , which defines the extent of any deviation from a trigonal-bipyramidal geometry ( $\tau = 1$  for a perfect trigonal bipyramidal and  $\tau = 0$  for a perfect square-based pyramid),<sup>11</sup> is calculated to be 0.85 (**Int2**–**C**–**Si**), 0.81 (**Int2**–**Si**–**Si**), 0.76 (**Int2**–**Ge**–**Si**), 0.74 (**Int2**–**Sn**–**Si**), and 0.63 (**Int2**–**Pb**–**Si**). It should be mentioned that these computed Si–N bond distances (1.997–1.945 Å) for the **Int2**–**E**–**Si** species are somewhat larger than values obtained by other studies of the five-coordinated silicon structures

(1.809–1.928 Å).<sup>12</sup> In addition, the increase in the atomic weight of the group 14 element **E** in the **Int2**–**E**–**Si** molecule causes a large increase in the Si–**E** and **E**–N bond distances, as already shown in the Supporting Information (Figure D).

(c) The expected product for the ring-expansion reaction of NHTs with  $\text{SiH}_2\text{Ph}_2$  is a six-membered heterocyclic compound that features two carbon atoms, two nitrogen atoms, one silicon atom, and one group 14 element **E**, as schematically outlined in the Supporting Information (Figure F). These computational results show that the reaction enthalpy increases as the atomic number of the group 14 element **E** increases. For instance, as shown in Table 2, the theoretical findings indicate that the Gibbs free reaction enthalpy (kcal/mol) for eq 1 increases in the order **Pro**–**C**–**Si** (–27) < **Pro**–**Si**–**Si** (+2.4) < **Pro**–**Ge**–**Si** (+7.7) < **Pro**–**Sn**–**Si** (+23) < **Pro**–**Pb**–**Si** (+37), but our theoretical results demonstrate that the energies of the ring-expansion products are all greater than those of their corresponding reactants, except for the case of carbon (**Rea**–**C**). This strongly implies that the ring-expansion reactions for heavy NHC species,

Table 3. Relative Energies (kcal/mol) for the Process Illustrated in Scheme 2<sup>a,b</sup>

system	E = C	E = Si	E = Ge	E = Sn	E = Pb
<b>Rea</b> -C + EH <sub>2</sub> Ph <sub>2</sub>	0.0	0.0	0.0	0.0	0.0
<b>TS1</b> -C-E ( $\Delta E_{\text{TS1}'}$ )	+99.7 (+85.9)	+35.7 (+20.6)	+39.9 (+26.2)	+34.1 (+23.1)	+40.7 (+29.6)
<b>Int1</b> -C-E ( $\Delta E_{\text{Int1}'}$ )	+7.55 (-6.69)	+4.15 (-9.22)	+4.13 (-7.73)	+6.26 (-6.09)	+4.99 (-8.38)
<b>TS2</b> -C-E ( $\Delta E_{\text{TS2}'}$ )	+38.5 (+25.3)	+28.6 (+15.1)	+30.9 (+19.2)	+32.9 (+18.3)	+35.0 (+23.8)
<b>Int2</b> -C-E ( $\Delta E_{\text{Int2}'}$ )	+62.8 (+49.4)	+13.8 (-0.176)	+20.3 (+7.03)	+21.1 (+9.65)	+28.8 (+16.0)
<b>TS3</b> -C-E ( $\Delta E_{\text{TS3}'}$ )	+69.8 (+55.4)	+21.4 (+7.24)	+34.8 (+20.8)	+31.1 (+20.9)	+43.7 (+32.2)
<b>Pro</b> -C-E ( $\Delta E_{\text{Pro1}'}$ )	+8.44 (-6.94)	-27.3 (-41.9)	-19.2 (-30.3)	-15.1 (-24.9)	-6.51 (-19.1)

<sup>a</sup>That is, **Rea**-C + EH<sub>2</sub>Ph<sub>2</sub> → **TS1**-C-E → **Int1**-C-E → **TS2**-C-E → **Int2**-C-E → **TS3**-C-E → **Pro**-C-E, calculated at the M06-2X/Def2-TZVP level of theory. For the M06-2X optimized structures of the stationary points, see the Supporting Information (Figures G–L). <sup>b</sup>Gibbs free energy and zero-point energy (in parentheses).

using SiH<sub>2</sub>Ph<sub>2</sub>, are mostly endothermic, which is energetically unfavorable. In other words, the heavy six-membered heterocyclic products **Pro**-E-Si (E = Si, Ge, Sn and Pb) are not produced from a SiH<sub>2</sub>Ph<sub>2</sub> molecule-insertion reaction, as represented in eq 1, but could possibly exist if these six-membered heterocyclic compounds are produced through other reaction paths.

(d) An intriguing model for interpreting the reactivity of the reactants is provided by the valence bond state correlation diagram (VBSCD) model, which is based on the work of Pross and Shaik.<sup>13,14</sup> It is thus concluded that both the order of the singlet and triplet states and their energy separation are responsible for the existence and the height of the energy barrier and for the reaction enthalpy.<sup>13,14</sup> This analysis used to explain the origin of the following observed trend:

The ring-expansion reaction for a *N*-heterocyclic carbene analogue (**Rea**-E + SiH<sub>2</sub>Ph<sub>2</sub> → **TS1**-E-Si → **Int1**-E-Si) that has a central atom E with a lower atomic number is more facile than that for a *N*-heterocyclic carbene analogue that has a central atom E with a greater atomic number.

The reason for this can be traced back to the singlet–triplet energy gap ( $\Delta E_{\text{st}}$ ) of a six-valence-electron *N*-heterocyclic carbene analogue (**Rea**-E). As discussed previously, the theoretical computations suggest that all of the reactants **Rea**-E have exclusively singlet ground states and that the energy  $\Delta E_{\text{st}}$  increases as the atomic mass of the group 14 element E increases. This result is also in accordance with the trend in the first activation energy ( $\Delta E_{\text{TS1}}$ ) and the first intermediate energy ( $\Delta E_{\text{Int1}}$ ) for eq 1. Accordingly, the theoretical findings strongly suggest that the  $\Delta E_{\text{st}}$  of a NHC analogue can be used as a diagnostic tool to predict the reactivity of various NHT analogues in ring-expansion reactions with different phenylsilanes.

Furthermore, in the first step of eq 1 (**Rea**-E + SiH<sub>2</sub>Ph<sub>2</sub> → **TS1**-E-Si → **Int1**-E-Si), one Si–H bond is broken, and two bonds are formed (E–Si and E–H). It was reported that the bond strengths for E–Si and E–H bonds decrease in the general order (kcal/mol) C–Si (82.7) > Si–Si (76.0) > Ge–Si (70.6) > Sn–Si (55.7) > Pb–Si (31.5)<sup>15</sup> and C–H (92.2) > Si–H (86.0) > Ge–H (78.8) > Sn–H (69.2) > Pb–H (57.8),<sup>16</sup> respectively. Again, these data are consistent with the trend in the first intermediate energy ( $\Delta E_{\text{Int1}}$ ) for eq 1. In consequence, this provides strong evidence that the larger the atomic weight of group 14 element E involved in the heavy NHC analogue (**Rea**-E), the longer are the E–Si and E–H bond distances, the weaker are the

E–Si and E–H bond strengths, and, in turn, the smaller is the enthalpy for the cleavage of the H–Si bond in SiH<sub>2</sub>Ph<sub>2</sub> of eq 1.<sup>17</sup>

**(3). Geometrical and Energetic Results for eq 2.** The other type of ring-expansion reaction, which contains the NHC species and various EH<sub>2</sub>Ph<sub>2</sub> (E = C, Si, Ge, Sn, and Pb) is also considered, namely, eq 2, which is calculated at the M06-2X/Def2-TZVP level of theory. As mentioned in Scheme 2, the mechanism for eq 2 is as follows: **Rea**-C + EH<sub>2</sub>Ph<sub>2</sub> → **TS1**-C-E → **Int1**-C-E → **TS2**-C-E → **Int2**-C-E → **TS3**-C-E → **Pro**-C-E. Although most of these reactions have not been experimentally investigated,<sup>1</sup> it is believed that the computational results presented in this work should provide information that is pertinent to future experimentation. The calculated reaction energetics are listed in Table 3 and Figure 3. In addition, the key geometrical parameters for these reactions are listed in the Supporting Information (Figures G–L). There are several noteworthy features of Figure 3, Table 3, and the Supporting Information (Figures G–L).

(a) From Table 3, it is easily seen that the atomic number of the atom E that is under attack in the heavy EH<sub>2</sub>Ph<sub>2</sub> systems causes a large increase in the energy barrier of the first step of eq 2 (**Rea**-C + EH<sub>2</sub>Ph<sub>2</sub> → **TS1**-C-E), particularly for the **TS1**-C-C point. That is, the Gibbs free barrier height (kcal/mol) for the E–H bond breaking process increases in the order **TS1**-C-Sn (34) < **TS1**-C-Si (36) < **TS1**-C-Ge (40) < **TS1**-C-Pb (41) ≪ **TS1**-C-C (100). In other words, the smaller the atomic number of the E center involved in the heavy EH<sub>2</sub>Ph<sub>2</sub> molecule, the larger is the hydrogen-insertion barrier. In particular, the reason for the very large activation energy in the case of **TS1**-C-C could be due to steric congestion between the **Rea**-C and CH<sub>2</sub>Ph<sub>2</sub> molecules and the electronic structures (vide infra).

(b) Similarly to eq 1, there are two possible intermediates, **Int1**-C-E and **Int2**-C-E, located in the reaction paths of eq 2, as illustrated in Figures H and J, respectively (Supporting Information). **Int1**-C-E features a five-membered ring skeleton, and **Int2**-C-E possesses a six-membered ring of chair form. The M06-2X/Def2-TZVP frequency calculations indicate that these intermediates are true minima, without the imaginary frequencies. Unfortunately, the experimental observations, as documented in ref 6, show that no intermediate has been found. Nevertheless, such a species may possibly be involved as an intermediate for the insertion reaction.

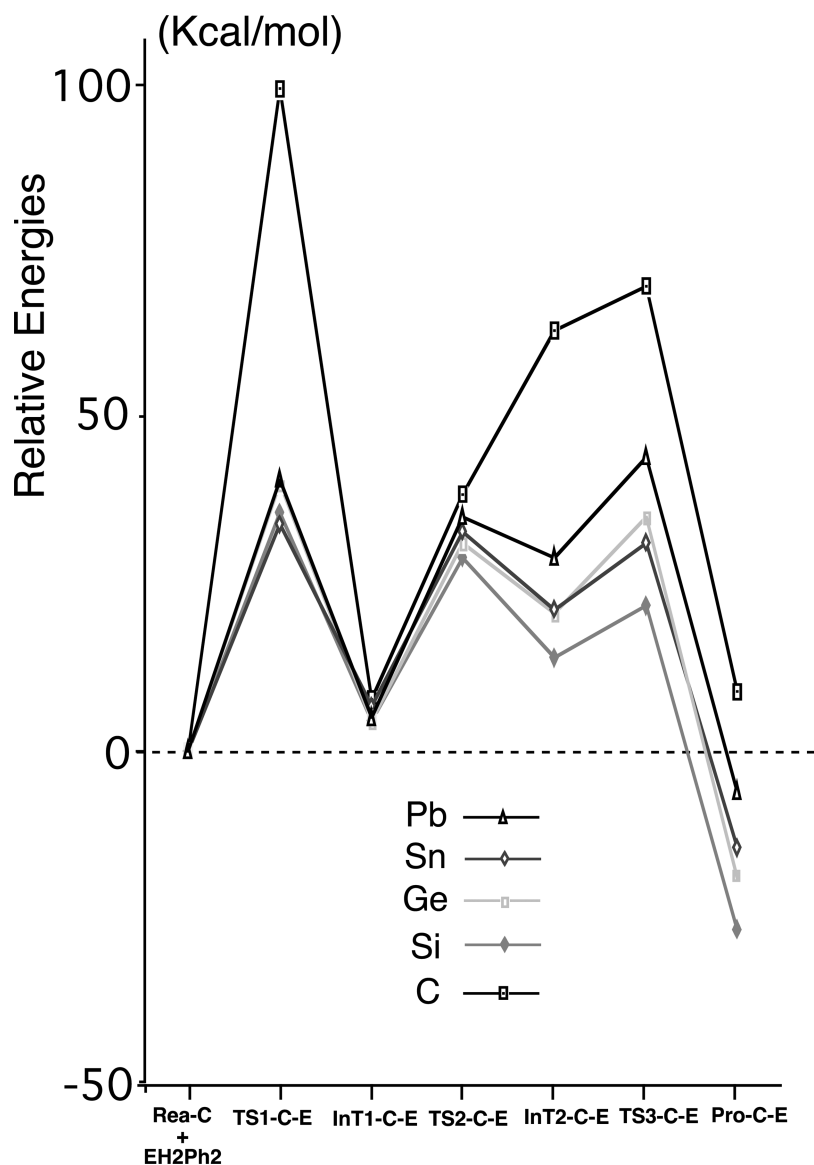


**Figure 3.** The potential-energy surfaces of the reactants **Rea-C** +  $\text{EH}_2\text{Ph}_2$ , transition states, intermediates, and ring-expansion products ( $\text{E} = \text{C}, \text{Si}, \text{Ge}, \text{Sn}, \text{and Pb}$ ), based on the M06-2X/Def2-TZVP calculations. For the relative Gibbs free energies for each species, see Table 3.

The most significant results are the structures of the intermediates **Int2-C-E**. As is seen in Figure J (Supporting Information), the group 14 element **E** is five-coordinate<sup>10</sup> and arranged in a distorted trigonal-bipyramidal geometry. Its coordination environment consists of three carbon atoms, one nitrogen atom, and a hydrogen atom. The two carbon atoms attached to the **E** atom originate from two phenyl ligands. According to the previous definition for the structural index  $\tau$ ,<sup>11</sup> these intermediates **Int2-C-E** are computed to be 0.61 (**Int2-C-C**), 0.89 (**Int2-C-Si**), 0.91 (**Int2-C-Ge**), 0.92 (**Int2-C-Sn**), and 0.88 (**Int2-C-Pb**). It should be emphasized that as already shown for the **Int2-C-C** of Figure J (Supporting Information), one C-C bond length in the six-membered ring is estimated to be 3.164 Å, which is considerably longer than experimentally determined C-C single bond distances (1.3–1.4 Å).<sup>3</sup> This strongly indicates that a van der Waals force exists between these two carbon atoms. This finding, again, is consistent with the traditional concept that the carbon atom can only form four chemical bonds with the other four groups. This long bond length is also reflected in the calculated energy.

As shown in Table 3, the free energy of the **Int2-C-C**, relative to its corresponding reactants, is approximately 63 kcal/mol, and its energy barrier to the next TS (**TS3-C-C**) is only approximately 7 kcal/mol. Moreover, since the computational results indicate that the relative energy of **Int2-C-C** is much higher than that of **TS2-C-C**, this intermediate should not appear in the addition reaction of **Rea-C** with  $\text{CH}_2\text{Ph}_2$ .

(c) The theoretical results depicted in Figure L (Supporting Information) show that all of the ring-expansion products **Pro-C-E** have a six-membered ring structure. Moreover, as demonstrated in Table 3, the energetic ordering of the ring-expansion product shows that the Gibbs free reaction enthalpy (kcal/mol) for the process is **Pro-C-Si** (−27) < **Pro-C-Ge** (−19) < **Pro-C-Sn** (−15) < **Pro-C-Pb** (−6.5) < **Pro-C-C** (+8.4), which shows that the energies of the ring-expansion products are all less than those of their corresponding reactants, except for the case of carbon (**Pro-C-C**). This strongly implies that the ring-expansion reaction for NHC species by  $\text{EH}_2\text{Ph}_2$  is exothermic, with the exception of  $\text{E} = \text{C}$ . Considering its energetically unfavorable five-coordinated intermediate **Int-C-C**, it can be concluded that

the six-membered heterocyclic product **Pro**-C-C cannot be a product of the ring-expansion reaction, as denoted in eq 2. However, it could possibly exist if **Pro**-C-C is produced via the other reaction route.

(d) Again, the VBSCD model can be used to explain the origin of the following observed trend:<sup>13,14</sup> for the insertion of NHC into the ring-expansion product, the reactivity of  $\text{EH}_2\text{Ph}_2$  decreases in the order  $\text{SiH}_2\text{Ph}_2 \approx \text{GeH}_2\text{Ph}_2 \approx \text{SnH}_2\text{Ph}_2 > \text{PbH}_2\text{Ph}_2 \gg \text{CH}_2\text{Ph}_2$ . The driving force for this can also be simply understood in terms of the singlet-triplet energy gap ( $\Delta E_{\text{st}}$ ) of  $\text{EH}_2\text{Ph}_2$ . The valence  $\sigma$  and  $\sigma^*$  MOs that are involved in the E-H bonds in the  $\text{EH}_2\text{Ph}_2$  species at the M06-2X/Def2-TZVP level are collected in Figure 4. The substitution of a single

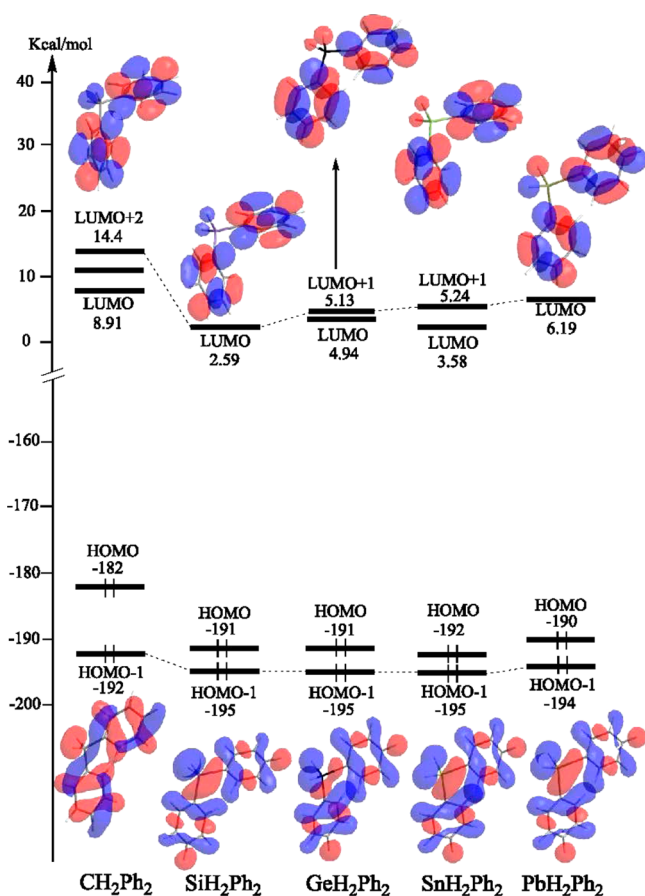


**Figure 4.** The  $\sigma$  and  $\sigma^*$  MOs for the  $\text{EH}_2\text{Ph}_2$  ( $E = \text{C}, \text{Si}, \text{Ge}, \text{Sn}, \text{and Pb}$ ) species concerning the E-H bonds.

E atom in the  $\text{EH}_2\text{Ph}_2$  molecule decreases the energy of the  $\sigma^*$  (E-H) orbital, on going from  $\text{CH}_2\text{Ph}_2$  to  $\text{PbH}_2\text{Ph}_2$ , while the energy of the  $\sigma$  (E-H) orbital remains comparatively constant. As a result, the DFT calculations indicate that the  $\Delta E_{\text{st}}$  for  $\text{CH}_2\text{Ph}_2$ ,  $\text{SiH}_2\text{Ph}_2$ ,  $\text{GeH}_2\text{Ph}_2$ ,  $\text{SnH}_2\text{Ph}_2$ , and  $\text{PbH}_2\text{Ph}_2$  are 206.7, 197.7, 199.9, 200.1, and 200.6 kcal/mol, respectively; that is,  $\Delta E_{\text{st}}$  increases in the order  $\text{SiH}_2\text{Ph}_2 < \text{GeH}_2\text{Ph}_2 < \text{SnH}_2\text{Ph}_2 < \text{PbH}_2\text{Ph}_2 < \text{CH}_2\text{Ph}_2$ . It is readily seen that this result is in accordance with the trends in activation energy and enthalpy ( $\Delta E_{\text{TS1}}$ ,  $\Delta E_{\text{int1}}$ ), given in Table 3. Consequently, these model calculations provide strong evidence that the electronic factor resulting from the  $\text{EH}_2\text{Ph}_2$  structure plays a decisive role in determining the reactivity of  $\text{EH}_2\text{Ph}_2$  in the ring-expansion reaction with a NHC.

## IV. CONCLUSION

Taking all of the heavy **Rea**-E and  $\text{EH}_2\text{Ph}_2$  ( $E = \text{C}, \text{Si}, \text{Ge}, \text{Sn}$ , and  $\text{Pb}$ ) systems and the two aforementioned reactions (eqs 1 and 2) studied in this paper together, the following conclusions can be drawn:

- (1) In the case of eq 1 (**Rea**-E +  $\text{SiH}_2\text{Ph}_2$ ), for a given  $\text{SiH}_2\text{Ph}_2$ , the reactivity of the **Rea**-E species toward the ring-expansion reaction decreases as the atomic weight of the central atom E increases; that is, the reactivity decreases in the order **Rea**-C  $\gg$  **Rea**-Si > **Rea**-Ge > **Rea**-Sn > **Rea**-Pb. That is to say, only **Rea**-C (i.e., NHC) can readily undergo concerted Si-H bond insertion and a ring-expansion reaction. However, the other heavy **Rea**-E ( $E = \text{Si}, \text{Ge}, \text{Sn}$ , and  $\text{Pb}$ ) systems undergo the ring-expansion reaction with  $\text{SiH}_2\text{Ph}_2$  with difficulty, since their activation barriers are quite high, and the entire reactions are endothermic. Indeed, it has been experimentally reported that only the **Rea**-C species can react with  $\text{SiH}_2\text{Ph}_2$  to undergo the ring-expansion reaction.<sup>1</sup>
- (2) In the case of eq 2 (**Rea**-C +  $\text{EH}_2\text{Ph}_2$ ), for a given **Rea**-C, the reactivity of the  $\text{EH}_2\text{Ph}_2$  molecule toward the ring-expansion reaction decreases in the order  $\text{SiH}_2\text{Ph}_2 \approx \text{GeH}_2\text{Ph}_2 \approx \text{SnH}_2\text{Ph}_2 > \text{PbH}_2\text{Ph}_2 \gg \text{CH}_2\text{Ph}_2$ . That is, **Rea**-C cannot undergo C-H bond insertion with  $\text{CH}_2\text{Ph}_2$ , and, in turn, no ring-expansion reaction occurs, since it is an energetically unfeasible process, from both a kinetics and thermodynamic viewpoint. The  $\text{SiH}_2\text{Ph}_2$  species is also the most likely to undergo the ring-expansion reaction with the **Rea**-C compound.
- (3) This work demonstrates that the computational results can be rationalized using a simple VBSCD model.<sup>13,14</sup> The concepts of the VBSCD model, which focuses on the singlet-triplet splitting ( $\Delta E_{\text{st}}$ ) in the reactants, allow the rapid estimation of the relative reactivity of a variety of **Rea**-E and  $\text{EH}_2\text{Ph}_2$  species, without specific knowledge of the actual energies of the interactions involved.<sup>18</sup>

It is ultimately hoped that the parameters presented in this paper will be a guide for any future experimental investigations.

## ■ ASSOCIATED CONTENT

### 📄 Supporting Information

This contains additional optimized geometries and atomic coordinates. This material is available free of charge via the Internet at <http://pubs.acs.org>.

## ■ AUTHOR INFORMATION

### ✉ Corresponding Author

\*E-mail: midesu@mail.ncyu.edu.tw.

### Notes

The authors declare no competing financial interest.

## ■ ACKNOWLEDGMENTS

The author is grateful to the National Center for High-Performance Computing of Taiwan for generous amounts of computing time. He also thanks the Ministry of Science and Technology of Taiwan for the financial support. Special thanks go to the reviewers for very helpful suggestions and comments.

## ■ REFERENCES

- (1) Schmidt, D.; Berthel, J. H. J.; Pietsch, S.; Radius, U. *Angew. Chem., Int. Ed.* **2012**, *51*, 8881.
- (2) For theoretical works, see: (a) Momeni, M. R.; Rivard, E.; Brown, A. *Organometallics* **2013**, *32*, 6201. (b) Iverson, K. J.; Wilson, D. J. D.; Dutton, J. L. *Organometallics* **2013**, *32*, 6209. (c) Iverson, K. J.; Wilson, D. J. D.; Dutton, J. L. *Dalton Trans.* **2013**, *42*, 11035. (d) Fang, R.; Yang, L.; Wang, Q. *Organometallics* **2014**, *33*, 53.
- (3) Recently, there are several experimental papers concerning the C–N bond activation and ring opening of a NHC compound. It was also reported that direct insertion of BeH<sub>2</sub> unit into a C–N bond of a NHC compound may be affected under mild conditions. For instance, see: (a) Arrowsmith, M.; Hill, M. S.; Kociok-Kohn, G.; MacDougall, D. J.; Mahon, M. F. *Angew. Chem., Int. Ed.* **2012**, *51*, 2140. (b) For similar work, one can also see Al-Rafia, S. M. I.; McDonald, R.; Ferguson, M. J.; Rivard, E. *Chem.—Eur. J.* **2012**, *18*, 13810. (c) Bose, S. K.; Fucke, K.; Liu, L.; Steel, P. G.; Marder, T. B. *Angew. Chem., Int. Ed.* **2014**, *53*, 1799. (d) Wang, T.; Stephan, D. W. *Chem.—Eur. J.* **2014**, *20*, 3036.
- (4) For N-heterocyclic silylenes, see (a) Denk, M.; Lennon, R.; Hayashi, R.; West, R.; Belyakov, A. V.; Verne, H. P.; Haaland, A.; Wangner, M.; Wetzler, N. *J. Am. Chem. Soc.* **1994**, *116*, 2691. (b) Denk, M.; Hayashi, R. K.; West, R. *J. Am. Chem. Soc.* **1994**, *116*, 10813. (c) Urquhart, S. G.; Hitchcock, A. P.; Lehmann, J. L.; Denk, M. *Organometallics* **1998**, *17*, 2352. (d) Haaf, M.; Schmiedl, A.; Schmedake, T. A.; Powell, D. R.; Millevolte, A. J.; Denk, M.; West, R. *J. Am. Chem. Soc.* **1998**, *120*, 12714. (e) Haaf, M.; Schmedake, T. A.; West, R. *Acc. Chem. Res.* **2000**, *33*, 704. (f) Asay, M.; Jones, C.; Driess, M. *Chem. Rev.* **2011**, *111*, 354. (g) Blom, B.; Gallego, D.; Driess, M. *Inorg. Chem. Front.* **2014**, *1*, 134.
- (5) For five-membered N-heterocyclic carbene analogues of the group 14 elements, see (a) Herrmann, W. A.; Denk, M.; Benk, M.; Behm, J.; Scherer, W.; Klingan, F.-R.; Bock, H.; Solouki, B.; Wagner, M. *Angew. Chem., Int. Ed.* **1992**, *31*, 1485. (b) Arduengo, A. J., III; Bock, H.; Chen, H.; Denk, M.; Dixon, D. A.; Green, J. C.; Herrmann, W.; Jones, N. L.; Wagner, M.; West, R. *J. Am. Chem. Soc.* **1994**, *116*, 6641. (c) Arduengo, A. J., III; Dias, H. V. R.; Dixon, D. A.; Harlow, R. L.; Klooster, W. T.; Koetzle, T. F. *J. Am. Chem. Soc.* **1994**, *116*, 6812. (d) Denk, M. K.; Hatano, K.; Lough, A. J. *Eur. J. Inorg. Chem.* **1998**, 1067. (e) Heitmann, D.; Pape, T.; Hepp, A.; Muck-Lichtenfeld, C.; Grimme, S.; Hahn, F. E. *J. Am. Chem. Soc.* **2011**, *133*, 11118. (f) Chen, J.-Y.; Su, M.-D. *Dalton Trans.* **2011**, *40*, 7898.
- (6) Frisch, M. J. et al. *Gaussian 09*; Gaussian, Inc.: Wallingford, CT, 2013.
- (7) Zhao, Y.; Truhlar, D. G. *Acc. Chem. Res.* **2008**, *41*, 157.
- (8) (a) Andrae, D.; Haeussermann, U.; Dolg, M.; Stoll, H.; Preuss, H. *Theor. Chim. Acta* **1990**, *77*, 123. (b) Metz, B.; Stoll, H.; Dolg, M. *J. Chem. Phys.* **2000**, *113*, 2563. (c) Peterson, K. A.; Figgen, D.; Goll, E.; Stoll, H.; Dolg, M. *J. Chem. Phys.* **2003**, *119*, 11113. (d) Leiminger, T.; Nicklass, A.; Kuechle, W.; Stoll, H.; Dolg, M.; Bergner, A. *Chem. Phys. Lett.* **1996**, *255*, 274. (e) Kaupp, M.; Schleyer, P. V.; Stoll, H.; Preuss, H. *J. Chem. Phys.* **1991**, *94*, 1360.
- (9) For instance, see Jacobsen, H.; Correa, A.; Poater, A.; Costabile, C.; Cavallo, L. *Coord. Chem. Rev.* **2009**, *253*, 687 and related references therein.
- (10) For instance, see Junold, K.; Baus, J. A.; Burschka, C.; Tacke, R. *Angew. Chem., Int. Ed.* **2012**, *51*, 7020 and related references therein.
- (11) (a) Addison, A. W.; Rao, T. N.; Reedijk, J.; van Rijn, J.; Verschoor, G. C. *Dalton Trans.* **1984**, 1349. (b) Chandrasekhar, V.; Azhakar, R.; Senapati, T.; Thilagar, P.; Ghosh, S.; Verma, S.; Boomishankar, R.; Steiner, A.; Kogerler, P. *Dalton Trans.* **2008**, 1150.
- (12) (a) Azhakar, R.; Ghadwal, R. S.; Roesky, H. W.; Granitzka, M.; Stalke, D. *Organometallics* **2012**, *31*, 5506. (b) Azhakar, R.; Propper, K.; Dittrich, B.; Roesky, H. W. *Organometallics* **2012**, *31*, 7586.
- (13) For details, see (a) Shaik, S.; Schlegel, H. B.; Wolfe, S. In *Theoretical Aspects of Physical Organic Chemistry*; John Wiley & Sons Inc.: Hoboken, NJ, 1992. (b) Pross, A. In *Theoretical and Physical Principles of Organic Reactivity*; John Wiley & Sons, Inc.: Hoboken, NJ, 1995. (c) Shaik, S. *Prog. Phys. Org. Chem.* **1985**, *15*, 197. (d) Shaik, S.; Hiberty, P. C. In *A Chemist's Guide to Valence Bond Theory*; Wiley, Interscience: Hoboken, NJ, 2008.
- (14) (a) For the paper that originated the VBSCD model, see Shaik, S. *J. Am. Chem. Soc.* **1981**, *103*, 3692. (b) About the most updated review of the VBSCD model, one can see Shaik, S.; Shurki, A. *Angew. Chem., Int. Ed.* **1999**, *38*, 586. (c) Hoffmann, R.; Shaik, S.; Hiberty, P. C. *Acc. Chem. Res.* **2003**, *36*, 750.
- (15) (a) Cottrell, T. L. In *The Strengths of Chemical Bonds*, 2nd ed.; Butterworths: London, U.K., 1981. (b) Becerra, R.; Walsh, R. In *The Chemistry of Organic Silicon Compounds*, Vol. 2; Rappoport, Z., Apeloig, Y., Eds.; Wiley: Chichester, U.K., 1998. (c) Ciccioli, A.; Gigli, G. *J. Phys. Chem. A* **2012**, *116*, 7107.
- (16) Temelso, B.; Sherrill, C. D.; Merkle, R. C.; Freitas, R. A., Jr. *J. Phys. Chem. A* **2007**, *111*, 8677.
- (17) Our conclusions are similar to those studied by Dutton, Wilson, and co-workers. That is, the relative bond enthalpies for E–H and C–H would be a possible driving force for the ring-expansion reaction studied in this work. See ref 7b,c.
- (18) We also calculated both eq 1 and eq 2 using the B3LYP/LANL2DZ+dp level of theory. Again, as can be seen in Table A and Table B (Supporting Information), the reactivity trends are quite similar to the corresponding ones based on the M06-2X/Def2-TZVP method. This strongly implies that the reactivity trends for the ring-expansion reactions of NHCs are conserved for different kinds of levels of theory.